

Bistability in atmospheric oxygen and the Great Oxidation

Colin Goldblatt*, Tim Lenton and Andy Watson

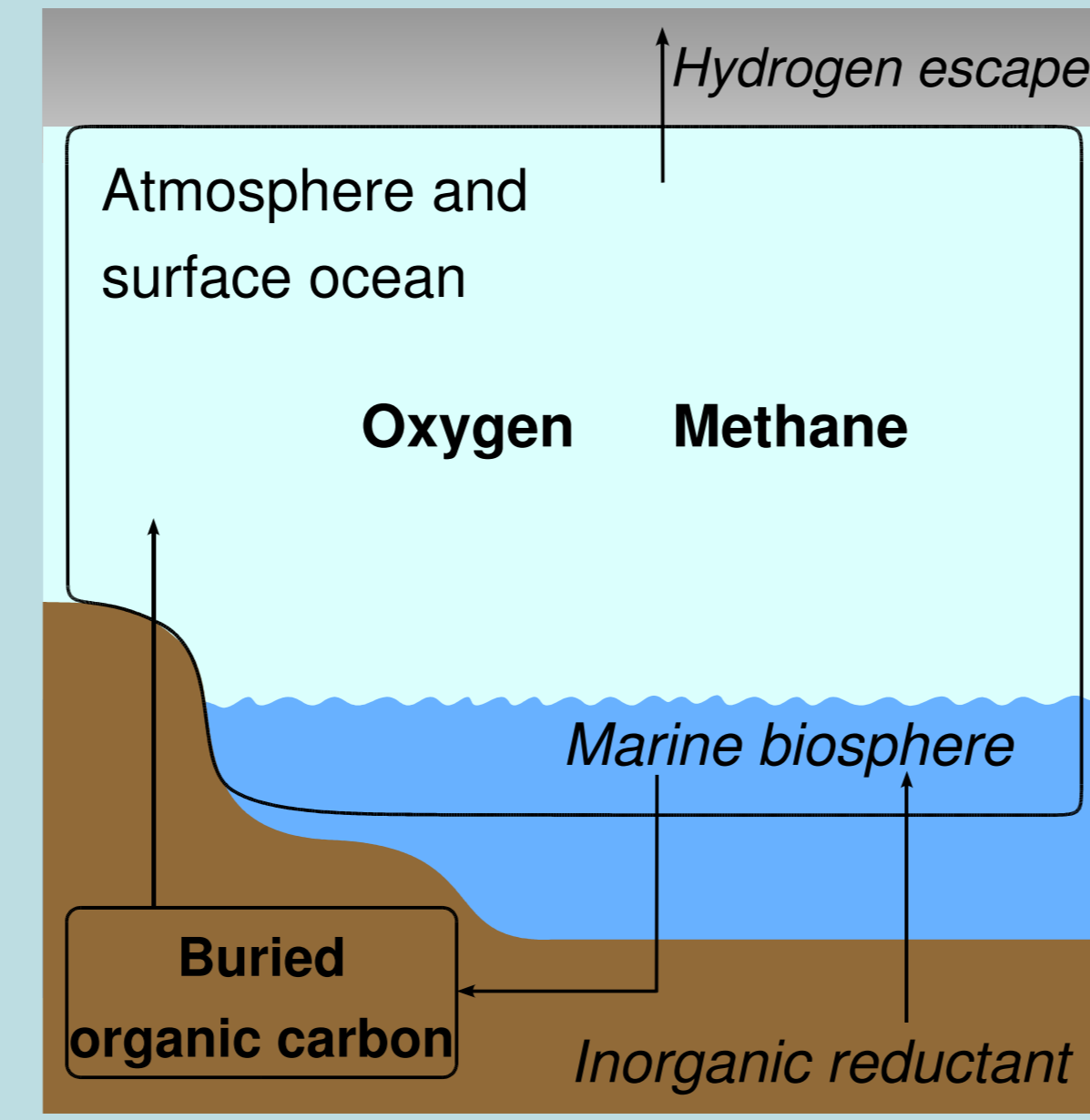
School of Environmental Sciences, University of East Anglia, Norwich, NR4 7TJ, U.K.

abstract

Earth history has been characterised by a series of major transitions separated by long periods of relative stability¹. Chemically the largest transition was the “Great Oxidation” at 2.4 Ga, when atmospheric oxygen rose from $< 10^{-5}$ PAL (Present Atmospheric Level) to > 0.01 PAL and possibly² > 0.1 PAL. This occurred long after the origin of oxygenic photosynthesis³⁻⁶, ≥ 2.7 Ga. The cause of this delay and the subsequent Great Oxidation are hotly debated⁷⁻¹². Here we show that the origin of oxygenic photosynthesis gave rise to two simultaneously stable steady states for atmospheric oxygen. The existence of a low oxygen ($< 10^{-5}$ PAL) steady state explains how a reducing atmosphere persisted for ≥ 300 million years after the origin of oxygenic photosynthesis. The Great Oxidation can be understood as a switch to the high oxygen ($> 5 \times 10^{-3}$ PAL) stable steady state. The bistability arises because ultraviolet shielding of the troposphere by ozone becomes effective once oxygen exceeds 10^{-5} PAL, causing a nonlinear increase in the lifetime of atmospheric oxygen. Our results show that the existence of oxygenic photosynthesis is not a sufficient condition for an oxygen rich atmosphere or the existence of an ozone layer, which has implications for detecting life on other planets by atmospheric analysis^{13, 14}.

a conceptual model

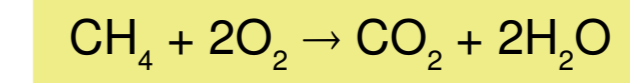
We have constructed a conceptual model of the global redox system following the advent of oxygenic photosynthesis with methane (M) and oxygen (O) in atmosphere and surface ocean and buried organic carbon in the crust (C).



Marine Biosphere

- Net primary productivity from oxygenic photosynthesis, N
- Net input of reductant to the surface, r (an electron donor for anoxygenic photosynthesis)
- Pathway for decomposition of organic matter depends on available oxygen: aerobic respiration with high oxygen, otherwise fermentation and methanogenesis
- Methane can be used by methane oxidising bacteria with sufficient oxygen.
- Oxygenic photosynthesis followed by fermentation and methanogenesis contributes both oxygen and methane to the atmosphere:
 $\text{CO}_2 + \text{H}_2\text{O} + \text{h}\nu \rightarrow \frac{1}{2}\text{CH}_4 + \frac{1}{2}\text{CO}_2 + \text{O}_2$
- $\Omega(\text{O}_2)$ is the fraction of productivity transferred to the atmosphere as methane and oxygen.

Atmospheric methane oxidation



- Takes place as a series of reactions, some are photochemically mediated.
- We parameterise this rate by fitting the results of detailed photochemical models³³⁻³⁵.
- $\Psi(\text{O}_2)$ is a polynomial function of oxygen concentration. Once the is enough oxygen an ozone layer forms, shielding the troposphere from UV radiation. This reduces the rate of photolysis of water which decreases OH availability, thus suppressing the rate of methane oxidation^{34, 36}.

Hydrogen escape is diffusion limited, with methane as the sole source of hydrogen in the upper atmosphere and s as a limiting flux constant.

$$\begin{aligned} \frac{dM}{dt} &= \frac{1}{2}\Omega(\text{O}_2)(N+r) - \frac{1}{2}\Psi(\text{O}_2) - sM - \frac{1}{2}\Omega(\text{O}_2)(\beta(N+r) - wC) \\ \frac{dO}{dt} &= \Omega(\text{O}_2)N - (1 - \Omega(\text{O}_2))r - \Psi(\text{O}_2)M^{0.7} - sM + (1 - \Omega(\text{O}_2))(\beta(N+r) - wC) \\ \frac{dC}{dt} &= \beta(N+r) - wC \end{aligned}$$

Buried organic carbon.

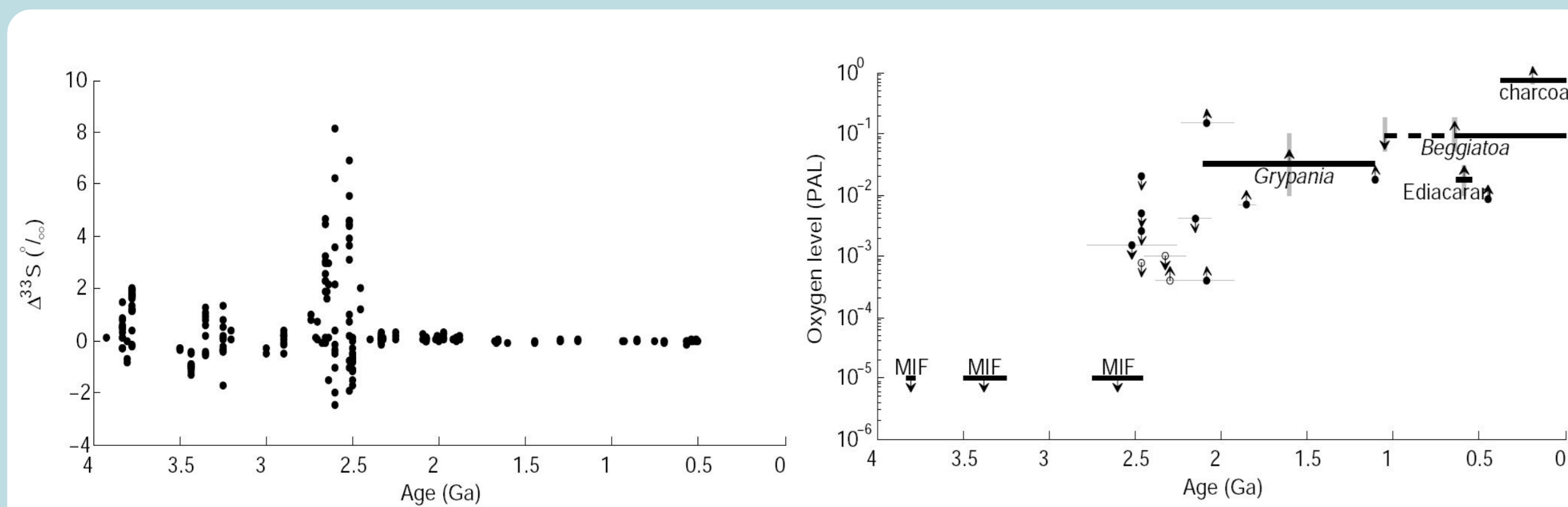
- Fraction β of ocean productivity is buried.
- Weathering rate w is determined mechanically.
- Exposed organic carbon is decomposed by organisms.

background

The Great Oxidation describes the rise of atmospheric oxygen from $< 10^{-5}$ PAL to > 0.01 PAL at 2.4 Ga.

- Before the origin of life, photochemical models¹⁵ predict $\text{O}_2 < 10^{-12}$ PAL.
- Evidence of mass independent fractionation (MIF) of sulphur isotopes¹⁶⁻²³ prior to 2.45 Ga, constrains²⁴ O_2 to $< 10^{-5}$ PAL. The MIF signal is absent in samples^{20, 23} 2.33 Ga and younger.
- Geological and biological constraints²⁵⁻²⁹, particularly palaeosols²⁵, indicate O_2 consistently > 0.01 PAL after 2.4 Ga, and possibly > 0.1 PAL.

Oxygenic photosynthesis originated ≥ 2.7 Ga, at least 300 million years before the Great Oxidation. The cause of this delayed oxidation is hotly debated^{7,9-12,30,32}. Recent hypotheses assume that the Great Oxidation will be triggered when the oxygen source exceeds the input of volcanic and metamorphic reductants^{7-10, 12}.



Constraints on palaeo-oxygen. **a** Compilation of evidence of MIF in sulphur isotopes for the Precambrian¹⁶⁻²³. Deviations from $\Delta 34\text{S} = 0$ indicate $\text{O}_2 < 10^{-5}$ PAL²⁴. Note the abrupt end of the strong MIF signal at 2.4 Ga. **b** Compilation of proxies for palaeo-oxygen. Upward arrow indicates lower bounds and downward arrows indicate upper bounds. Solid black lines are duration of the constraint. Dashed black line means that oxygen is thought to have crossed the given threshold in that time. Grey lines are error bars. Circles represent palaeosols²⁵. The oxygen constraint for these is from an $\text{O}_2 : \text{CO}_2$ ratio and assumed pCO_2 ; these constraint would be affected by any change from the assumed pCO_2 . Open circles are weakly constrained. Ediacaran²⁶ is a constraint from the oxygen demand of fauna in this period, Beggiatoia refers to oxygen constraints from this organism together with changes in the sulphur cycle²⁹. Charcoal requires sufficient oxygen for combustion²⁹.

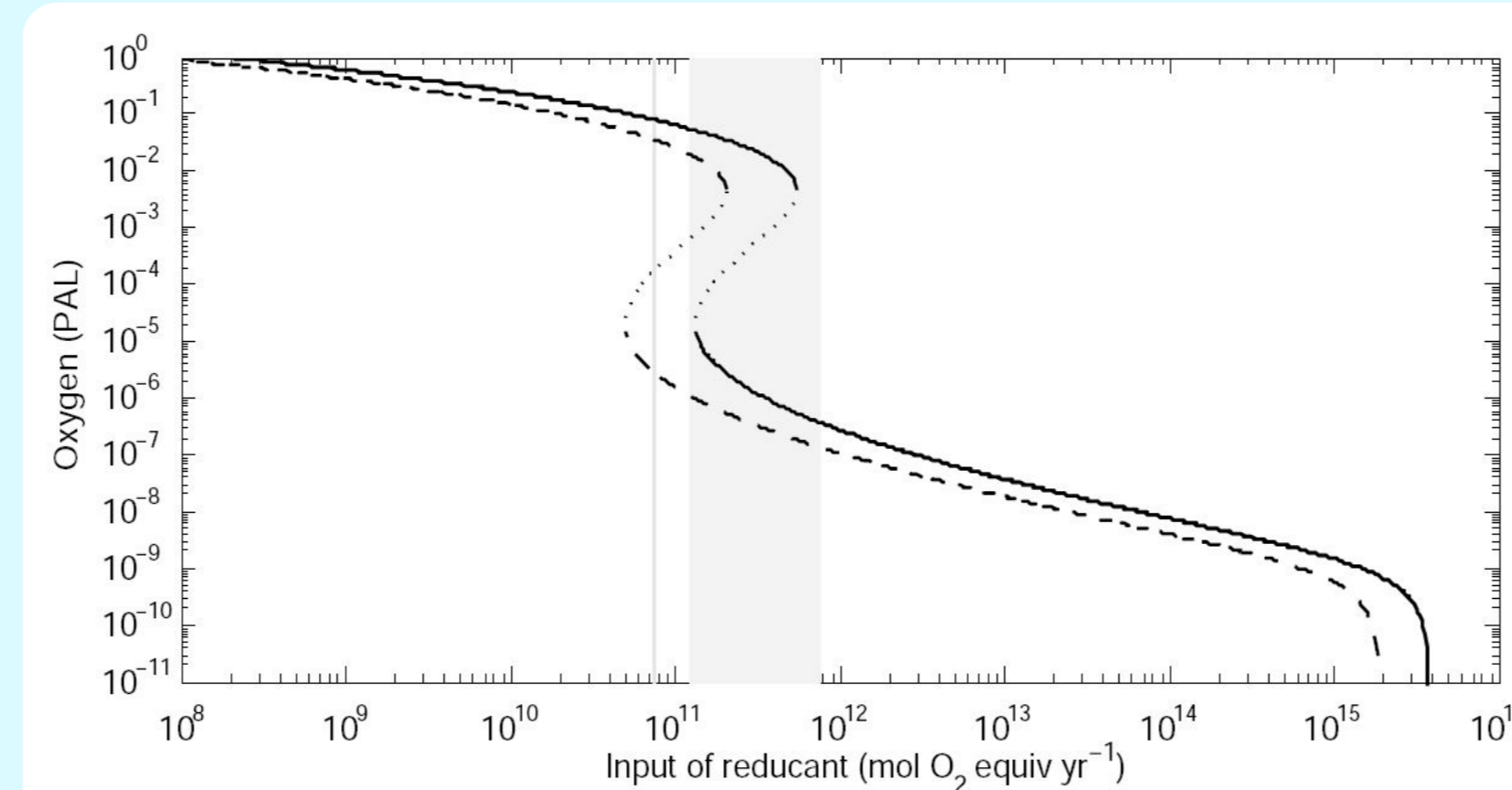
results

The steady state solutions for methane and carbon are

$$M = \frac{r}{s} \quad C = \frac{\beta(N+r)}{w}$$

and the solutions for oxygen are the roots of

$$\Omega(\text{O}_2)N - (1 - \Omega(\text{O}_2))r - \Psi(\text{O}_2)\left(\frac{r}{s}\right)^{0.7} - s\left(\frac{r}{s}\right) = 0$$



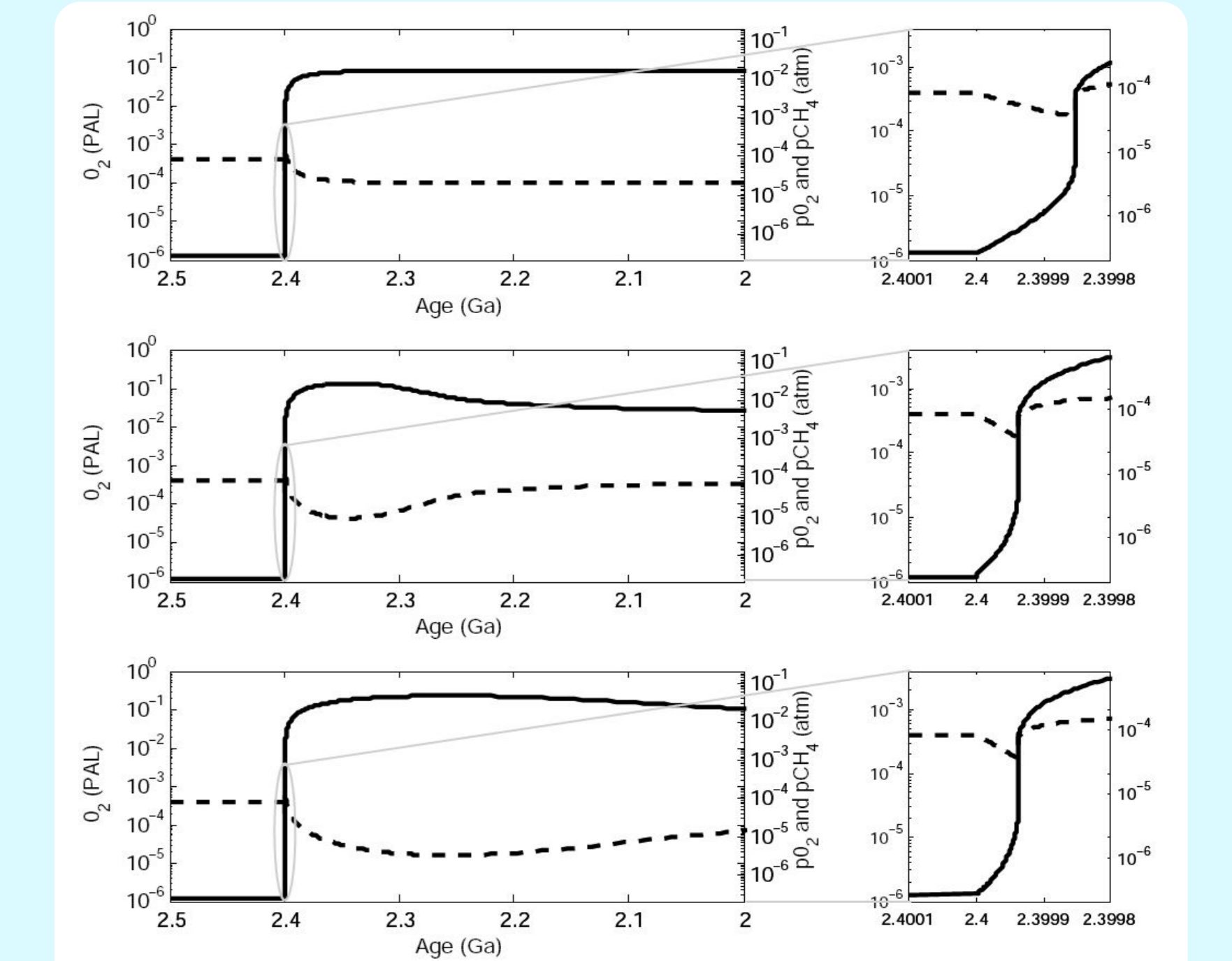
Steady state solutions for oxygen with respect to reductant input to the surface. Stable steady state solutions are shown with solid and dashed lines, unstable steady states with dotted lines. Solid line for modern marine NPP and dashed line with half of present NPP for comparison. Shaded area shows constraints on iron deposition in BIFs before the great oxidation which is taken as a proxy for reductant input³⁷. Vertical grey line shows the present hydrothermal input of Fe to the ocean³⁸.

Thus we explain the dynamics of the Great Oxidation:

- **There is a bistability in atmospheric oxygen.**
- **The low oxygen stable steady state for oxygen explains the prolonged existence of reduced conditions after the origin of oxygenic photosynthesis.**
- **The Great Oxidation was the switch between the two stable steady states for oxygen.** This could have happened in response to a small change in forcing.
- **The bistability arises from the formation of an ozone layer.** When there is sufficient oxygen an ozone layer forms, this increases photochemical lifetime of oxygen, enhancing ozone formation. Positive feedback on oxygen.
- **The Great Oxidation occurred when oxygen exceeded 10^{-5} PAL,** which is the threshold for ozone layer development. This contrasts with previous assumptions that it occurred when the oxygen source from carbon burial exceeded the input of reduced material.
- **The likely trigger for the Great Oxidation was a decrease in reductant input to the surface.** This is indicated by a large decrease in banded iron formations (BIF) deposition at the time⁸, probably due to the end of a mantle superplume event³⁷. Alternatively, a transient increase in oxygen production from increased carbon burial could have caused the switch between bistable states.

Wider implications

Our results are relevant to the search for life on other planets by atmospheric analysis. It has been assumed that a planet which hosts oxygenic photosynthesis should have high oxygen and an ozone layer. The low oxygen stable steady state in the presence of oxygenic photosynthesis suggests that low oxygen, and no ozone layer, could continue indefinitely



Transient Runs. Response of oxygen and methane in our model to step changes at 2.4 Ga representing possible triggers of the Great Oxidation. **a** decrease in reductant input, r from 3×10^{11} to 7.5×10^{10} mol O_2 equiv. yr^{-1} inferred from decreased BIF deposition^{27, 37}; **c** does not change significantly. **b** 5% increase in net primary productivity, N ; **c** increases by 5% over ~ 500 million years after the oxidation. **c** Combined decrease in r and 2% increase in N ; **c** increases by 2% over ~ 500 million years after the oxidation.

c.goldblatt@uea.ac.uk

* Also Centre for Ecology and Hydrology, Bush Estate, Penicuik, Midlothian, EH26 0QB, U.K.



1. Lenton, T., Coleson, K. & Sefton, A. E. What does history teach us about the major transitions and rate of disturbance in the evolution of life and the Earth system. In: *Sustainability*, H. Cruzan, P. Clark, W. Clausen, M. & Held, H. (eds.) Earth Systems Analysis for Sustainability, vol. 91 of *Durham Working Reports*, 29-52 (MIT Press, Cambridge, Mass., 2004).

2. Holland, W. D. The oxygenation of the atmosphere and oceans. *Philos. Trans. R. Soc. B* (in Press).

3. Brooks, J. J., Logan, G. A., Burch, R. & Semoren, R. Archean molecular fossils and the early rise of eukaryotes. *Science* 285, 1035-1038 (1999).

4. Burch, R. The antiquity of oxygenic photosynthesis - evidence from stromatolites in sulfatedepleted Archean lakes. *Science* 285, 1474-1477 (1999).

5. Stroop, J. W. Microfossils of the early Archean report chart - new evidence of the antiquity of life. *Science* 260, 640-646 (1993).

6. DesMarais, D. J. When did photosynthesis emerge on Earth. *Science* 288, 1703-1705 (2000).

7. Holland, W. D. Volcanic gases, black smokers, and the great oxidation event. *Geochim. Cosmochim. Acta* 66, 3011-3021 (2002).

8. Barley, M. E., Bekker, A. & Kröner, B. Late Archean to early Paleoproterozoic global tectonics, environmental change and the rise of atmospheric oxygen. *Earth Planet. Sci. Lett.* 238, 150/171 (2005).

9. Kump, L. R., Kasting, J. F. & Barley, M. E. Rise of atmospheric oxygen and the “oxidation” of Archean metals. *Geochim. Cosmochim. Acta* 67, 1029-1030 (2003).

10. Kasting, J. F. The rise of atmospheric oxygen. *Science* 253, 819-820 (2001).

11. Catling, D., Zahnle, K. & McKay, C. Biogenic methane, hydrogen escape, and the irreversible oxidation of early Earth. *Science* 293, 839-843 (2001).

12. Catling, D. C. & Charn, M. W. How Earth’s atmosphere evolved to anoxic state: a status report. *Earth Planet. Sci. Lett.* 237, 1-20 (2005).

13. Lovelock, J. A physical basis for the detector experiments. *Nature* 207, 588 (1965).

14. Lovelock, J. & Lovelock, G. J. Life detection by atmospheric analysis. *Isaacs* 7, 148-159 (1967).

15. Kasting, J. F., Liu, S. C. & Donahue, T. M. Oxygen levels in the prebiological atmosphere. *J. Geophys. Res.* 94, 3071-3107 (1979).

16. Johnson, D. et al. Active microbial sulfur disproportionation in the Mesoproterozoic. *Science* 289, 757-759 (2000).

17. Oros, S. et al. New insights into Archean sulfur cycle from mass-independent sulfur isotope records from the Hamlet basin, Australia. *Earth Planet. Sci. Lett.* 212, 15-30 (2003).

18. Hu, G., Rumble, D. & Wang, P.-X. An elevated laser temperature for the in situ analysis of multistep sulfur isotopes and its use in measuring Archean sulfur isotope mass-independent anomalies. *Geochim. Cosmochim. Acta* 67, 3101-3117 (2003).

19. Mojzsis, S., Coath, C., Greenwood, J., McKeegan, K. & Harrison, T. Mass-independent sulfur isotope effects in Archean (2.6 to 2.8 Ga) sedimentary sulfides determined by ion microprobe analysis. *Geochim. Cosmochim. Acta* 67, 1635-1658 (2003).

20. Kasting, J. F., Liu, S. C. & Donahue, T. M. Oxygen levels in the prebiological atmosphere. *J. Geophys. Res.* 94, 3071-3107 (1979).

21. Johnson, D. et al. Active microbial sulfur disproportionation in the Mesoproterozoic. *Science* 289, 757-759 (2000).

22. Pagniez, D., Mojzsis, S., Coath, C., Karhu, J. & McKeegan, K. Multiple sulfur isotope of sulfides from sediments in the aftermath of Paleoproterozoic glaciations. *Geochim. Cosmochim. Acta* 69, 5033-5040 (2005).

23. Oros, S., Bekker, N., Rumble, D. & Fogel, M. Early evolution of atmospheric oxygen from multiple sulfur and carbon isotope records of the 2.9 Ga Mozan group of the Pongola. *Geochim. Cosmochim. Acta* 67, 3101-3117 (2003).

24. Pavlov, A. A., Kasting, J. F., Brown, L. L., Reges, K. A. & Friedman, R. Greenhouse warming by CH4 in the atmosphere of early Earth. *J. Geophys. Res.* 105, 11481-11490 (2000).

25. Liu, Z.-X. & Li, G.-C. The consistency of upper mantle O2 through time inferred from V/Sr ratios in basalts. *Earth Planet. Sci. Lett.* 238, 445-453 (2004).

31. Karhu, J. A. & Holland, H. D. Carbon isotopes and the rise of atmospheric oxygen. *Geology* 24, 867-870 (1996).

32. Kopp, R. E., Kravchik, J. L., Hultin, I. A. & Nash, C. Z. The paleoproterozoic snowball Earth: a climate disaster triggered by the evolution of oxygenic photosynthesis. *Proc. Natl. Acad. Sci. U.S.A.* 102, 11511-11516 (2005).

33. Carlisle, D. & Teske, A. Late Proterozoic rise in atmospheric oxygen concentration inferred from phylogenetic and sulfur isotope studies. *Nature* 392, 157-161 (1999).

34. Pavlov, A., Hargrett, M., Kasting, J. F. & Arthur, M. Methane-rich Proterozoic atmosphere? *J. Geophys. Res.* 106, 22027-22037 (2001).

35. Liu, Z.-X. & Li, G.-C. The consistency of upper mantle O2 through time inferred from V/Sr ratios in basalts. *Earth Planet. Sci. Lett.* 238, 445-453 (2004).

36. Kopp, R. E., Kravchik, J. L., Hultin, I. A. & Nash, C. Z. The paleoproterozoic snowball Earth: a climate disaster triggered by the evolution of oxygenic photosynthesis. *Proc. Natl. Acad. Sci. U.S.A.* 102, 11511-11516 (2005).

37. Isley, A. E. & Abbott, D. H. Plume-related mafic volcanism and the deposition of banded iron formation. *J. Geophys. Res.* 104, 15461-15477 (1999).

38. Kasting, J. F. & Donahue, T. The evolution of the atmosphere. *cosmos*. *J. Geophys. Res.* 85, 3055-3063 (1980).